

## Top-quark search in multijet signals

F. A. Berends and J. B. Tausk

*Instituut-Lorentz, University of Leiden, P.O. Box 9506, 2300 RA Leiden, The Netherlands*

W. T. Giele

*Fermi National Accelerator Laboratory, P.O. Box 500, Batavia, Illinois 60510*

(Received 31 August 1992)

We investigate the possibilities of finding the top quark at the Fermilab Tevatron  $p\bar{p}$  collider ( $\sqrt{s} = 1.8$  TeV) in the lepton plus multijet signal. The theoretical uncertainties in the normalization of the top-quark production cross section and background signals make it important to look for the top quark in a final state where the top-quark mass is reconstructible from the final state. The  $W + 4$  jet final state offers a simple and direct way to reconstruct the top-quark mass through final-state invariant masses. It is shown that from a theoretical viewpoint the top quark is easily recovered from this  $W + 4$  jet cross section. The only limitation comes from the experimental ability to correctly reconstruct the invariant masses which might contain multiple jets.

PACS number(s): 13.85.Qk, 12.38.Bx, 13.87.Ce, 14.80.Dq

### I. INTRODUCTION

The present direct top-quark mass limit of  $m_{\text{top}} > 91$  GeV from the Collider Detector at Fermilab (CDF) Collaboration used an integrated luminosity of roughly  $5 \text{ pb}^{-1}$  [1]. Based on indirect constraints obtained from the standard model using a combination of measurements, in particular the combined data from the CERN  $e^+e^-$  collider LEP [2], the top mass is likely to be in the range  $m_{\text{top}} = 132^{+45}_{-50}$  GeV. This means the current collider run at Fermilab, yielding at least  $25 \text{ pb}^{-1}$  of integrated luminosity, should produce enough events to establish the existence of the top quark.

Given the above top-quark mass limit and expected top mass, the dominant production process of the top quarks is direct  $t\bar{t}$  production. The top quark will subsequently decay into a  $b$  quark and a  $W$  boson, resulting in the following signatures that can be used in the top search:

$$p\bar{p} \rightarrow t\bar{t} \rightarrow b\bar{b}W^+W^- \rightarrow b\bar{b}jjjj, \quad (1.1)$$

$$p\bar{p} \rightarrow t\bar{t} \rightarrow b\bar{b}W^+W^- \rightarrow b\bar{b}l\nu jj, \quad (1.2)$$

$$p\bar{p} \rightarrow t\bar{t} \rightarrow b\bar{b}W^+W^- \rightarrow b\bar{b}l\nu l'\nu', \quad (1.3)$$

where  $j$  denotes the jet originating from the hadronic  $W$  decays. Other authors have investigated single top-quark production [3], but that does not yield promising results for the Fermilab collider. We shall denote the various channels by the number of hard isolated charged leptons in the event.

The highest event rate is given by the zero lepton process (1.1) with its relative branching fraction of  $(\frac{2}{3}) \times (\frac{2}{3})$ . Unfortunately, this multijet final state suffers from a huge quantum chromodynamics (QCD) background and seems only usable when one of the  $b$  jets can be tagged. Even then, the background is still much larger than the signal. We refer to Refs. [4] and [5] for a more detailed discussion.

The single lepton channel (1.2) has a smaller event rate

with a relative weight of  $2 \times (\frac{2}{3}) \times (\frac{2}{3})$  (counting both electron/positron and muon/antimuon final states). However, the QCD background is strongly reduced by the presence of the isolated lepton, making it possible to get a signal-over-background ratio of order one. The main purpose of the present paper is to study this one-lepton signature and its background in more detail than in Ref. [6]. In particular, it will be shown how specific distributions can greatly improve the extraction of the signal. Depending on the mass difference of the top and the  $W$ -vector boson, the signal (1.2) can show up as one lepton with 2, 3, or 4 jets. With an increasing number of jets the calculation of the exact background cross section

$$p\bar{p} \rightarrow W + n \text{ jets} \quad (1.4)$$

becomes more and more involved. The  $n=3$  case was considered in Refs. [7] and [8] and the  $n=4$  in Ref. [6]. Some discussion of top signal versus background was given in Ref. [6] and also in Ref. [9], but in the latter, a shower Monte Carlo program was used to estimate (1.4) and not determine the exact evaluation. All the results for the single-lepton channel in this paper refer to the sum of  $e^+$  and  $e^-$  signals. For muons the results are, of course, the same.

The unlike two-lepton channel (1.3) only gives a contribution of  $2 \times (\frac{1}{3}) \times (\frac{1}{3})$  (not taking  $\tau$  leptons into account). The remainder consists of more difficult final states involving  $\tau$  leptons, electron-positron or muon-antimuon pairs.

The two-lepton signal has the clear advantage of a low background. It has been discussed in detail in Ref. [9]. However, because of the presence of two neutrinos, it is not possible to reconstruct the top mass. For a top search in this signal one has to rely on the event rates and compare them directly with the theoretically calculated  $t\bar{t}$  cross section. This results in a top mass with a theoretical error which is not known. These theoretical uncer-

tainties are discussed in detail in Sec. II. The usefulness of the signal will increase when accompanying jets are measured, but it will become clear that for the discovery of the top quark the study of the one-lepton signature in addition to the two-lepton signature is crucial.

The outline of the paper is as follows. In Sec. II the production cross sections and their uncertainties are discussed. In Sec. III some methods to determine the top mass which are not sensitive to the absolute value of the cross sections are proposed. Section IV presents the conclusions.

## II. THE PRODUCTION CROSS SECTION AND BACKGROUNDS

With the use of theoretical calculations, the most important consideration is the expected uncertainty in the answer due to the fixed-order perturbative calculation. For the top production both signal and background have their uncertainties that affect the applicability of the calculation. In general, the correlations between the final-state jets and leptons are already predicted well by leading-order calculations provided one uses the usual jet definitions. However, the normalization of the cross sections is uncertain due to the choice we have to make for the renormalization and factorization scales. One chooses the value for this scale close to the natural scale in the problem in order to minimize the uncalculated higher-order contributions. For top production this scale is around the top mass; for the background the scale is around the  $W$  mass.

In order to see the sensitivity to the renormalization

scale  $\mu$  which is a measure for the theoretical uncertainty due to the fixed-order calculation we make three choices: (1)  $M_W, m_{\text{top}}$ , respectively; (2)  $\frac{1}{2}M_W, \frac{1}{2}m_{\text{top}}$ ; (3)  $2\sqrt{M_W^2 + p_{T,W}^2}, 2\sqrt{m_{\text{top}}^2 + p_{T,t}^2}$ , where  $p_{T,W}$  is the transverse momentum of the  $W$  and  $p_{T,t}$  is the average of the transverse momenta of the two tops. The results are given in Fig. 1 for the single lepton plus jet final state. The solid lines correspond with the first scale choice, the dashed lines with the second (upper) and third (lower line). Both signal and background are leading-order estimates of the cross section. The jet definitions and kinematical cuts used are given in Table I. Note that the signal and background are comparable up to a top mass of around 150 GeV only when one demands that the final state contain both a lepton and four jets.

The normalization uncertainty in the background is relatively unimportant when we use distributions. However, in the two-lepton signal the ability to predict the theoretical cross section as a function of the top mass is crucial. From Fig. 2 it is clear that using the leading-order prediction for

$$p\bar{p} \rightarrow t\bar{t} \quad (2.1)$$

has a large uncertainty and would make it virtually impossible to determine the top mass using the two-lepton signal, which relies on the total cross section. However, for process (2.1) also the next-to-leading-order contributions have been calculated [10]. The next-to-leading-order cross section has a reduced sensitivity to the renormalization/factorization scale choices. This is demonstrated in Fig. 3, where we show the scale choice

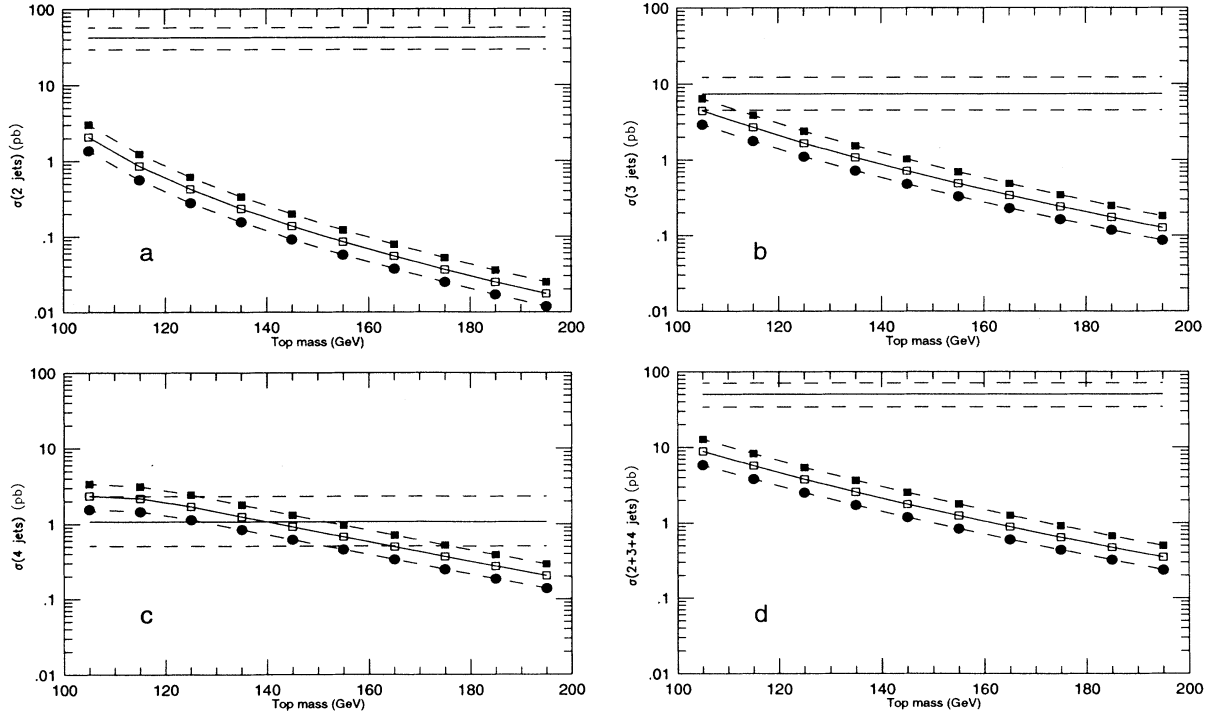


FIG. 1. (a), (b), and (c). The cross sections for  $p\bar{p} \rightarrow \text{lepton} + 2, 3,$  and  $4$  jets, respectively. The curves show the  $t\bar{t}$  signal, the horizontal lines are the QCD background. (d) shows the total  $p\bar{p} \rightarrow \text{lepton} + \text{jets}$  cross sections.

TABLE I. Parameters and cuts used for the one-lepton signal and background. For the two-lepton signal and background the same parameters and cuts are used, except that no cut is imposed on the missing momentum.

$\sqrt{s}$	1800 GeV
Structure function	MRS(B)
Jet rapidity coverage	2
Leptonic rapidity coverage	2
$E_t^{\min}$ (jet)	15 GeV
$E_t^{\min}$ (lepton)	20 GeV
$E_t^{\min}$ (missing)	20 GeV
Jet-jet separation $\Delta R$	0.7
Jet-lepton separation	None

sensitivity with the same choices as in leading order. For comparison, we also plotted the leading-order result with the same choices. One could now in principle use the next-to-leading-order calculation with its much smaller theoretical uncertainty to relate the value of the cross section to the top mass. However, in view of the large corrections to the Born cross sections, which amount to about 30%, one should worry about even higher-order contributions. The latter can be approximated by calculating the soft gluon corrections, which has been done in the literature [11]. If we apply this technique to approximate the next-to-leading-order contribution, we recover the exact next-to-leading-order result within about 10% (see Fig. 4), well within the theoretical uncertainty. Now we can apply the soft-gluon approximation to obtain an estimate of the next-to-next-to-leading-order contribution; this still gives a large positive correction of 25%. The results are summarized in Fig. 5, from which it is clear that the estimate of the theoretical uncertainty by changing the scale is not a good method for this particular cross section due to the large corrections. In fact, in Ref. [11] the soft-gluon effects are calculated to all orders in  $\alpha_s$ . For the  $q\bar{q}$  subprocess the resummed cross section is about the same size as the  $O(\alpha_s^2)$ -corrected cross sec-

tion, but for the  $gg$  subprocess the higher-order corrections are large and not well under control.

There are two other uncertainties affecting the top cross section. One results from the parton distribution functions, especially the gluon distribution function. The fraction of the  $t\bar{t}$  production that arises from gluon fusion ranges from about 50% for  $m_{\text{top}} = 100$  GeV through 28% for  $m_{\text{top}} = 140$  GeV to about 14% for  $m_{\text{top}} = 190$  GeV. To show the effect this has, we calculated the cross sections for (2.1) using two different sets of structure functions (see Fig. 6). The two sets of structure functions used are the Martin-Roberts-Stirling set B [MRS(B)] structure functions [12] with  $\Lambda_4 = 122$  MeV and the B1 set of structure functions for the modified minimal subtraction (MS) scheme in [13] with  $\Lambda_4 = 126$  MeV. The other uncertainty is a nonperturbative effect resulting from the Coulomb singularity. Its effect on the total cross section is less than 10% [14].

All the above effects give the predicted next-to-leading-order cross section a relatively large uncertainty. Therefore, the top-mass determination through the two-lepton final state, which relies on the ability to predict the cross section as a function for the top mass, has a larger uncertainty than one might expect from simple renormalization scale changes. The present CDF limit on  $m_{\text{top}}$  is based on a next-to-leading-order calculation that gives a cross section of 156 pb for  $m_{\text{top}} = 91$  GeV. In view of the above uncertainties, this limit also contains uncertainties. For instance, taking the next-to-next-to-leading-order approximation of the cross section literally would increase the  $m_{\text{top}}$  limit to 95 GeV. This is based on the value of the  $O(\alpha_s^2)$  corrected cross section of 155 pb at  $m_{\text{top}} = 95$  GeV. This clearly demonstrates that the top-mass determination is strongly sensitive to the absolute cross-section prediction.

### III. DETERMINATION OF THE TOP MASS

As we have shown in the preceding section, there will be problems when one relies on the absolute theoretical

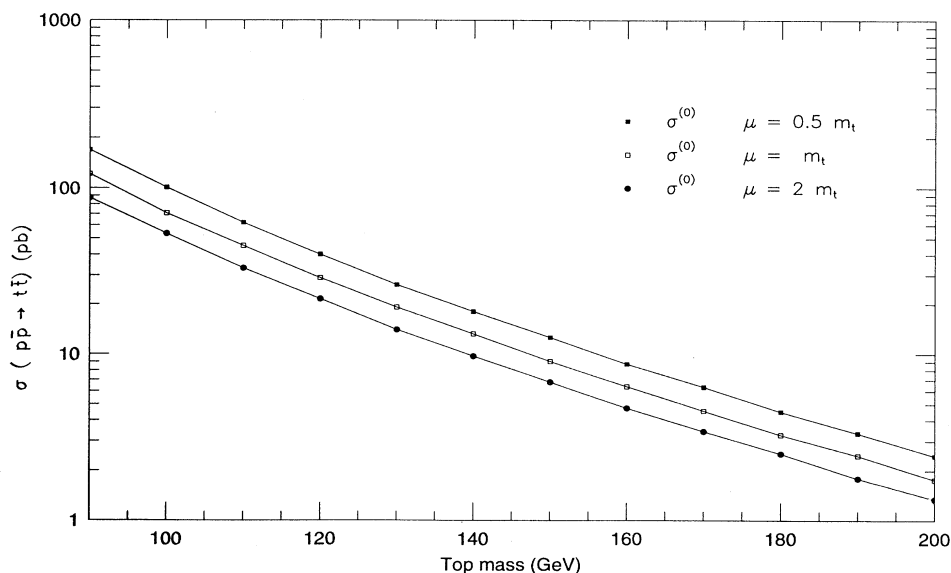


FIG. 2. The Born approximation to the total  $p\bar{p} \rightarrow t\bar{t}$  cross section using the MRS(B) structure functions for several choices of the renormalization scale  $\mu$ .

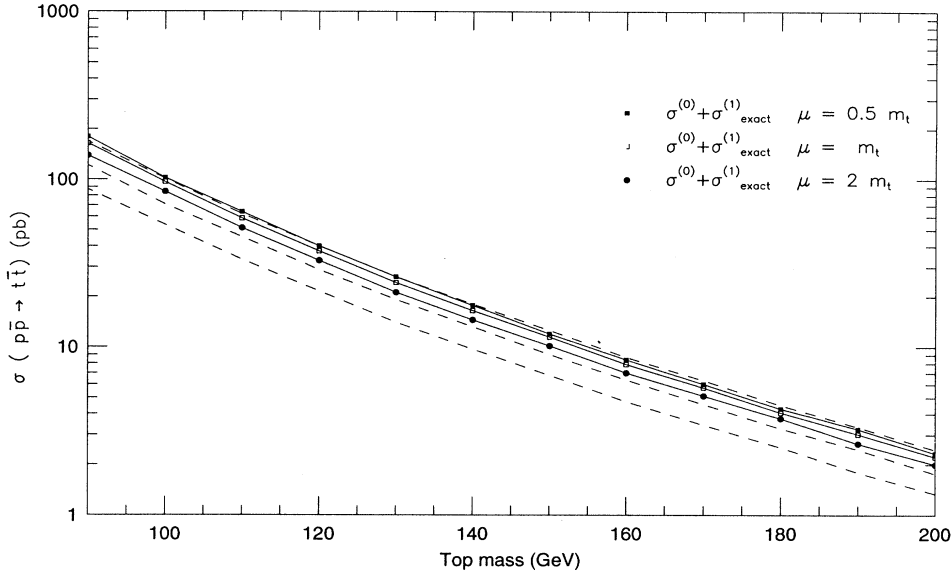


FIG. 3. Solid lines: the next-to-leading-order  $p\bar{p} \rightarrow t\bar{t}$  cross section using the MRS(B) structure functions. Dashed lines: the Born cross section.

prediction of the signal to determine the top mass. Therefore, we will explore in this section a few possible methods of circumventing these uncertainties.

The jet definitions and other kinematical cuts used throughout this section are listed in Table I. Note that one could apply additional cuts to improve the signal-over-background ratio (see, for instance, Ref. [16] where, in the case of the hadronic decay of the  $W$ , a cut is placed on the two-jet invariant mass). Also changing the jet definitions could improve the signal-over-background ratio [e.g. increasing the  $E_t^{\min}(\text{jet})$ ]. However, all these types of additional cuts or changes in the cuts will reduce the number of top events in the final sample and could increase experimental uncertainties. Therefore, one should apply them only when needed. As we will show, using the minimal set of cuts listed in Table I, which are dictated by detector properties, one already gets very reasonable results.

The first method uses the fact that the signal can have various numbers of jets in the final state. Differentiating between these jet final states enables us to form ratios of cross sections with different numbers of jets. In the approximation that the top is produced on shell, the production cross section (2.1) factorizes with respect to the subsequent decay of the top and cancels in the ratio; thus, the uncertainties in the production process are removed. Because the energy of the  $b$  quark is strongly related to the top mass, there will be a strong dependence in the jet fractions and ratios on the top mass. However, this way to cancel the normalization uncertainty in the top cross section only works when the background is negligible. This means the method can only be applied to the two-lepton signal and not the single-lepton-plus-multijets signal. By measuring the 0, 1, or 2 jets arising from energetic  $b$  quarks in the top pair decay, we can define jet fractions  $f_0$ ,  $f_1$ , and  $f_2$  by

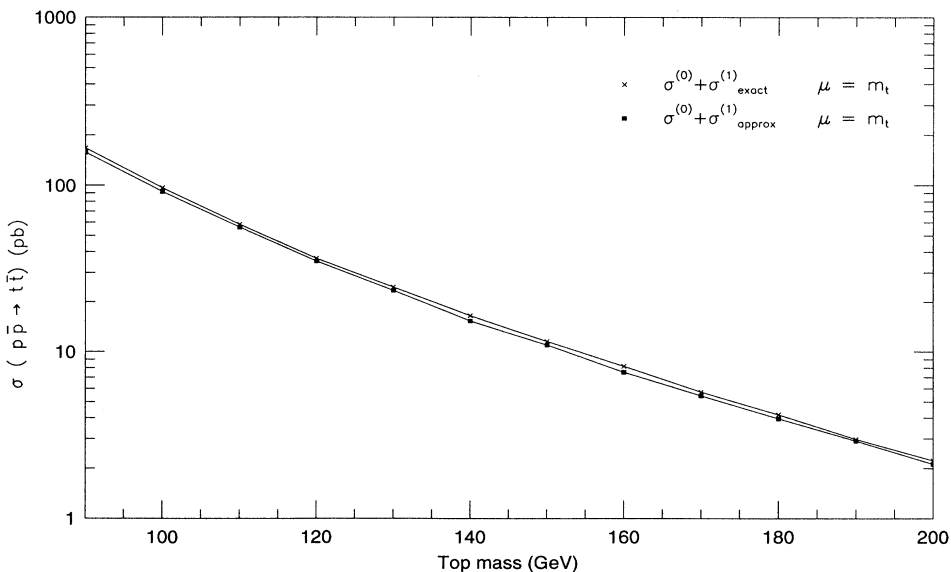


FIG. 4. A comparison of the exact next-to-leading-order  $p\bar{p} \rightarrow t\bar{t}$  cross section and the soft-gluon approximation using the MRS(B) structure functions.

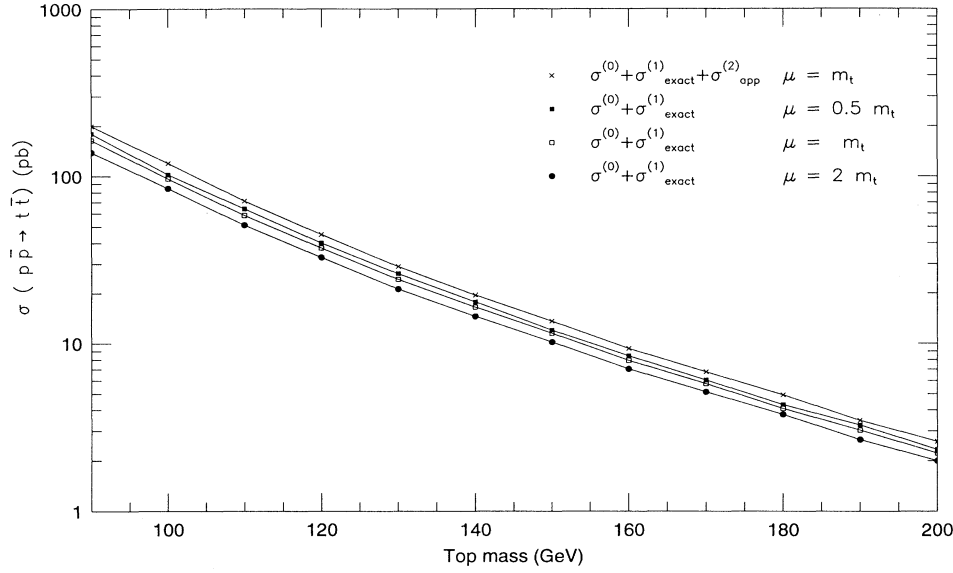


FIG. 5. The total  $p\bar{p} \rightarrow t\bar{t}$  cross section using the MRS(B) structure functions. The top curve includes the  $O(\alpha_s^2)$  contribution in the soft-gluon approximation; the other curves are the exact  $O(\alpha_s)$  corrected cross sections for the three choices of the scale  $\mu$ .

$$f_i = \frac{\sigma_i}{\sigma_0 + \sigma_1 + \sigma_2}, \quad (3.1)$$

where  $\sigma_i$  is the cross section for  $p\bar{p} \rightarrow 2$  leptons +  $i$  jets. As can be seen from Fig. 7, these fractions have a marked top-mass dependence, while there is almost no dependence on the scale. A measurement of such fractions gives an indication of the top mass without relying on the absolute event rates.

If one wants to use a jet fraction method in the single-lepton-plus-jets channel, the background has to be reduced to a negligible contribution. This, in fact, can be accomplished by  $b$  tagging for the three- and four-jet signals. It reduces the background by a factor for 50 for three jets and 30 for four jets while leaving the top cross section virtually unaffected. Thus, the ratio for the three- and four-jet rates is again a useful tool.

The single-lepton-plus-multijets final state offers a more direct possibility of determining the top mass. This is because the top mass is reconstructible from the final state using distributions. Possible uncertainties in the event rates are relatively unimportant provided that the signal-to-background ratio is of order unity. In Ref. [15] several distributions were examined in the lepton-plus-three-jet final state. However, the lepton-plus-four-jet final state offers a better possibility, since the signal-to-background ratio is expected to be much more favorable (see Fig. 1).

In order to extract the top mass from the signal, we will use two simple directly measurable quantities, the three-jet invariant mass and the cluster mass. Using the momentum of one of the four jets, the momentum of charged lepton, and the missing transverse momentum, the cluster mass is defined as

$$m_c(j, l; \nu)^2 = [p_T^0(jl) + p_T(\nu)]^2 - [\mathbf{p}_T(jl) + \mathbf{p}_T(\nu)]^2, \quad (3.2)$$

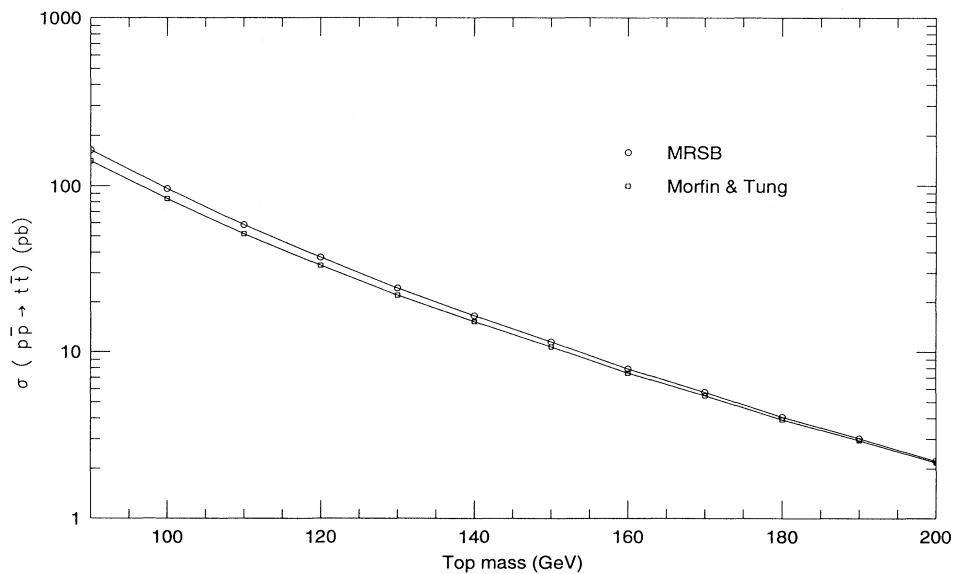


FIG. 6. The total  $O(\alpha_s)$  corrected  $p\bar{p} \rightarrow t\bar{t}$  cross section using two different sets of structure functions.

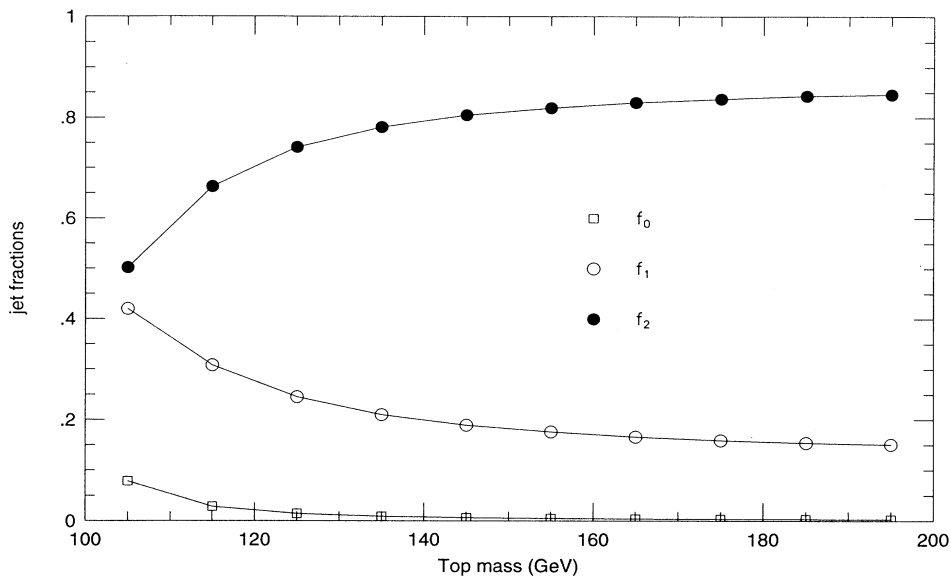


FIG. 7. The fractions of all  $p\bar{p} \rightarrow t\bar{t} \rightarrow 2$  leptons + jets events with 0, 1, and 2 jets.

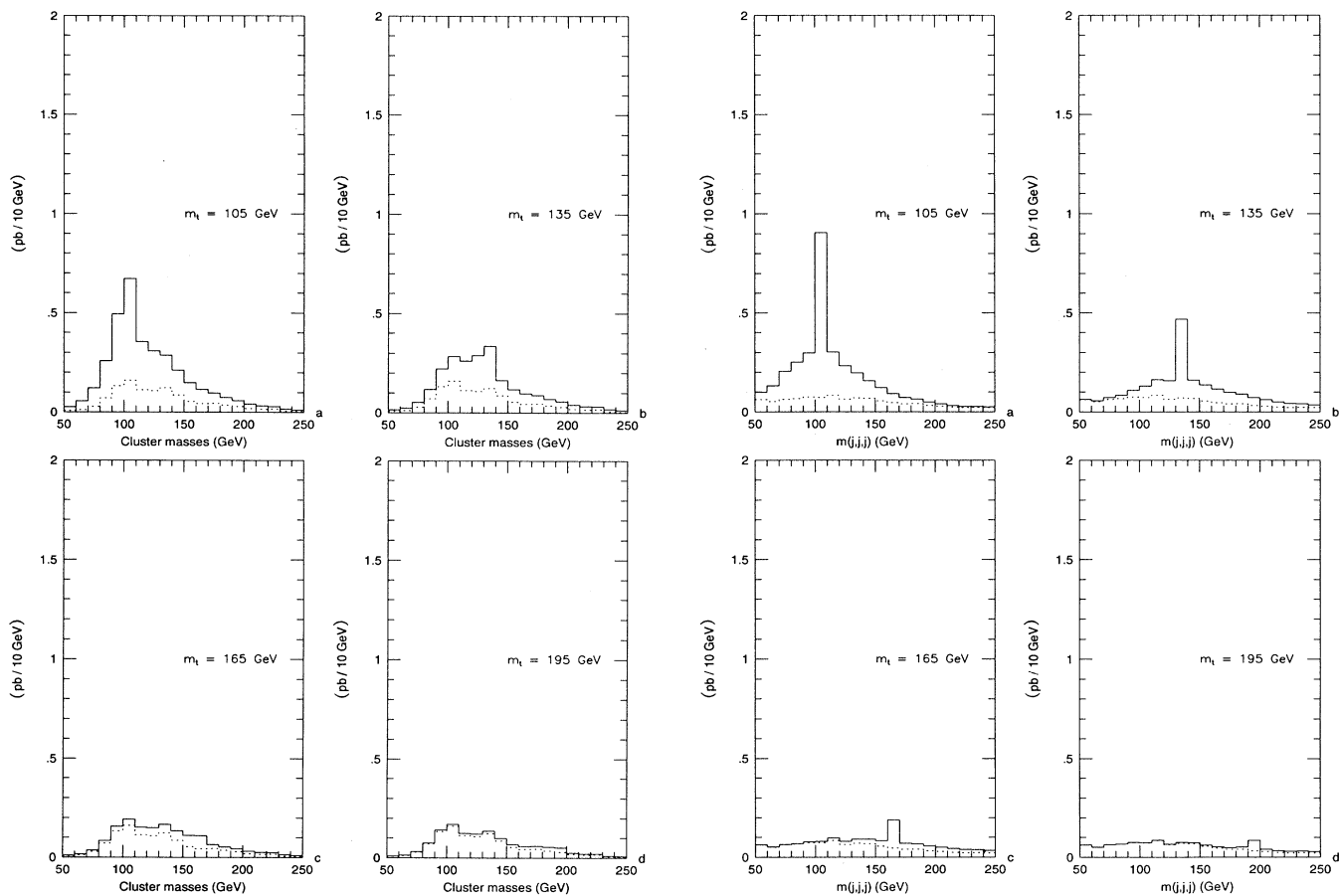


FIG. 8. Cluster-mass distributions for four values of  $m_{top}$ . The solid lines show the signal plus the background; the dotted lines show the background contribution.

FIG. 9. Three-jet-mass distributions for four values of  $m_{top}$ . The solid lines show the signal plus the background; the dotted lines show the background contribution.

where

$$p_T^0(jl) = \sqrt{\mathbf{p}_T(jl)^2 + m(jl)^2}, \quad (3.3)$$

$$\mathbf{p}_T(jl) = \mathbf{p}_T(j) + \mathbf{p}_T(l), \quad (3.4)$$

$$m(j_1, j_2, j_3) = \sqrt{[E(j_1) + E(j_2) + E(j_3)]^2 - [\mathbf{p}(j_1) + \mathbf{p}(j_2) + \mathbf{p}(j_3)]^2}. \quad (3.6)$$

All the following calculations are performed with scale 1. The results refer to the sum of the  $e^+$  and  $e^-$  signals. In Fig. 8 the average cluster-mass distributions (one entry for each of the four possible cluster masses) are shown due to signal and background. The histogram due to background alone is indicated with a dotted line. Four top-mass cases are presented: 105, 135, 165, and 195 GeV. For the latter two cases the top mass is not visible anymore; for the others a sharp drop indicates the top-mass position.

A better signal is obtained by using the three-jet mass distributions that are shown in Fig. 9 for both signal and background. Again, the background contribution is

$$m(jl)^2 = [E(j) + E(l)]^2 - [\mathbf{p}(j) + \mathbf{p}(l)]^2. \quad (3.5)$$

The three-jet mass is defined using the momenta of three of the four jets:

given by the dotted histogram. Above a top mass of 165 GeV the top signal is too small with respect to the background, making the peak virtually invisible.

We can easily improve these invariant mass distributions by using more of the kinematics of the top events. The cluster masses and the three-jet masses can be grouped into pairs, each consisting of a cluster mass calculated from one-jet momentum and a three-jet mass calculated from the three *other* momenta. By selecting the pair in each event in which the cluster mass and the three-jet mass are closest in value, two additional distributions are obtained. Each event gives one entry in a cluster-mass histogram and one in a three-jet mass histo-

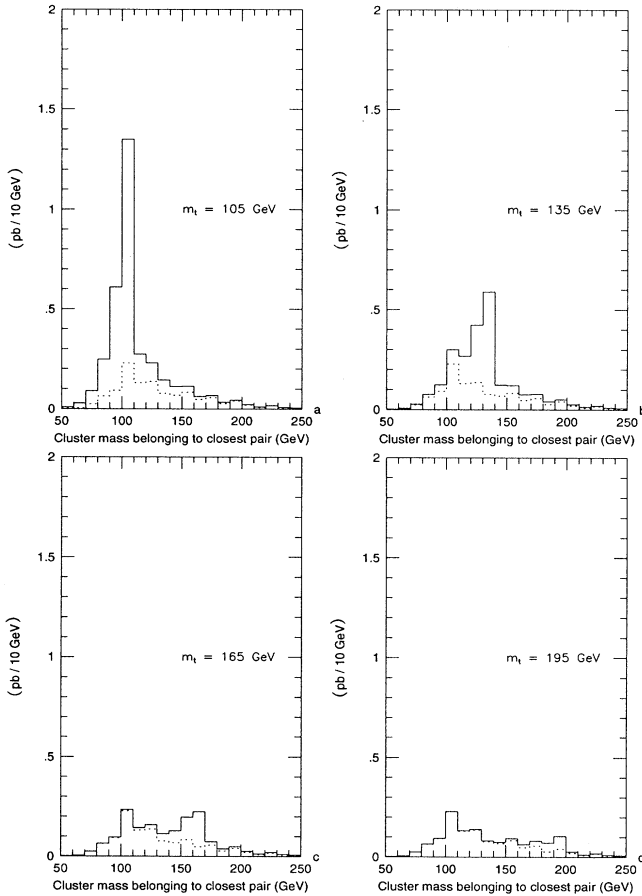


FIG. 10. The distribution of the cluster mass belonging to the selected pair for four values of  $m_{\text{top}}$ . The solid lines show the signal plus the background; the dotted lines show the background contribution.

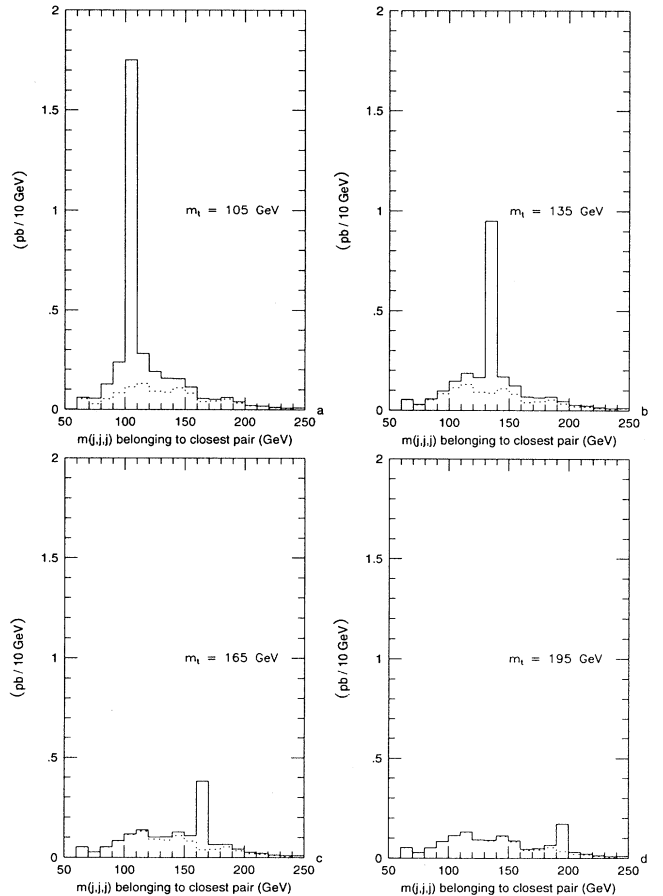


FIG. 11. The distribution of the three-jet mass belonging to the selected pair for four values of  $m_{\text{top}}$ . The solid lines show the signal plus the background; the dotted lines show the background contribution.

gram. The signals improve dramatically in these distributions. This can be seen in Figs. 10 and 11.

With this algorithm we also studied other top-mass values. Up to 160 GeV the top signal remains clearly visible, especially in the constrained three-jet mass (Fig. 11). Of course, no experimental detector effects are taken into account. The distributions shown would be the result when one uses the true jets and leptons, not affected by the detector acceptance. Determination of the top mass using these invariant masses is straightforward and direct, leaving no doubt whether or not there is a top or what its mass is.

#### IV. CONCLUSIONS

In this paper we have shown that the one-lepton-plus-four-jets channel is crucial for establishing the top quark.

With this signal it becomes possible to study distributions where the top reveals itself by a clear peak at the top mass. Of course, the experimental resolution will modify the shapes, but *a priori* the signal shows up above the background. The advantage of this method is that the top-mass determination is straightforward, making analysis of the theoretical and experimental uncertainties simple. Of course, the use of a distribution makes it necessary to require a reasonable number of events. With an integrated luminosity of  $25 \text{ pb}^{-1}$ , one can expect of the order of 50 events in this channel for a top-mass around 135 GeV, making this method applicable.

#### ACKNOWLEDGMENT

The research of J.B.T. was supported by the Stichting FOM.

- 
- [1] F. Abe *et al.*, Phys. Rev. Lett. **68**, 447 (1992).
  - [2] The LEP Collaborations: ALEPH, DELPHI, L3, and OPAL, Phys. Lett. B **276**, 247 (1992).
  - [3] R. K. Ellis and S. Parke, Phys. Rev. D **46**, 3785 (1992).
  - [4] Z. Kunszt and W. J. Stirling, Phys. Rev. D **37**, 2439 (1988).
  - [5] W. T. Giele, D. A. Kosower, and H. Kuijf, in *QCD '90*, Proceedings of the International Workshop, Montpellier, France, 1990, edited by S. Narison [Nucl. Phys. B **23B**, 22 (1991)].
  - [6] F. A. Berends, H. Kuijf, B. Tausk, and W. T. Giele, Nucl. Phys. **B357**, 32 (1991).
  - [7] K. Hagiwara and D. Zeppenfeld, Nucl. Phys. **B313**, 560 (1989).
  - [8] F. A. Berends, W. T. Giele, and H. Kuijf, Nucl. Phys. **B321**, 39 (1989).
  - [9] H. Baer, V. Barger, and R. J. N. Phillips, Phys. Rev. D **39**, 3310 (1989).
  - [10] P. Nason, S. Dawson, and R. K. Ellis, Nucl. Phys. **B303**, 607 (1988); W. Beenakker, H. Kuijf, W. L. van Neerven, and J. Smith, Phys. Rev. D **40**, 54 (1989).
  - [11] E. Laenen, J. Smith, and W. L. van Neerven, Nucl. Phys. **B369**, 543 (1992).
  - [12] A. D. Martin, R. G. Roberts, and W. J. Stirling, Phys. Lett. B **206**, 327 (1988).
  - [13] J. G. Morfin and W. K. Tung, Z. Phys. C **52**, 13 (1991).
  - [14] V. Fadin, V. Khoze, and T. Sjöstrand, Z. Phys. C **48**, 613 (1990).
  - [15] W. T. Giele and W. J. Stirling, Nucl. Phys. **B343**, 14 (1990).
  - [16] P. Agrawal and S. D. Ellis, Phys. Lett. B **221**, 393 (1989).